

## STATUS OF SELECTIVE EMITTER TECHNOLOGY

G. Hahn

University of Konstanz, Department of Physics, P.O. Box X916, 78457 Konstanz, Germany  
giso.hahn@uni-konstanz.de, Tel.: +49 7531 88 3644, Fax: +49 7531 88 3895

**ABSTRACT:** Current industrial monocrystalline Cz Si solar cells based on screen-printing technology for contact formation and homogeneous emitter have an efficiency potential of around 18.4%. Apart from limitations at the rear side by the fully covering Al-BSF the front side is limiting e.g. by relatively high  $j_{0E}$  values. This can be changed by selective emitter designs allowing a decoupling and separate optimization of the metalized and non-metalized areas. Several selective emitter concepts that are already in industrial mass production or close to it are presented, and their specialties and status concerning cell performance are demonstrated. Key issues to be considered are cost-effectiveness, added complexity, additional benefits, reliability, and efficiency potential. The efficiency increase for best cells is around 0.5-0.6%<sub>abs</sub> and the current efficiency potential already demonstrated for all technologies is around 19.0%. Average efficiencies in industrial mass production for selected technologies are 18.5-18.6% for Cz and 17.1% for mc Si.

The efficiency increase by selective emitter formation is higher for inline emitters, but selective emitters based on  $\text{POCl}_3$  show the highest absolute efficiency. By decreasing the phosphorous surface concentration, selective emitters are more sensitive to surface passivation and the use of a  $\text{SiN}_x\text{:H}$  layer with a higher refractive index increases implied  $V_{oc}$  values even further. Encapsulation under module glass and EVA reduces part of the gained  $j_{sc}$  caused by a better blue response on cell level, but a calculation reveals that this extra loss for selective emitter solar cells is  $<0.1 \text{ mA/cm}^2$  and therefore negligible. The full benefit of the improved front side in terms of a selective emitter structure will be achieved when local rear contacts will be used.

Keywords: c-Si, Selective Emitter, Screen Printing

## 1 INTRODUCTION

While the global photovoltaic (PV) market is booming and the Si shortage of the last years is currently no issue anymore, solar cell producers have to concentrate on the cost per  $W_p$  of their product, especially as the competition between the manufacturers becomes more and more important. Therefore, most cell manufacturers try to optimize their solar cell processes concerning higher efficiencies while not significantly increasing costs.

On several roadmaps the change from a homogeneous towards a selective emitter (SE) design is high on the list. Apart from this, the development of an alternative to the fully covering Al back-surface-field (BSF) on the rear side promises higher efficiencies as well. At the moment the latter approach seems to be more difficult to realize in an industrial way for various reasons (e.g. cost, contact design, throughput, yield), therefore the realization of a selective emitter design for standard screen-printed crystalline Si solar cells is the short-term goal in industry.

This paper will give an overview on various selective emitter technologies which are currently ready for industrial implementation or very close to it. As not for all technologies free information is available, this review will be restricted to technologies where information is available from recent publications.

## 2 SELECTIVE EMITTERS

## 2.1 Current status of homogeneous emitter technology

The standard industrial solar cell process in the last years is shown in Fig. 1 on the right. After a phosphorous diffusion (around  $50\text{-}60 \Omega/\text{sq}$ ) the P-glass is removed and a hydrogen-rich  $\text{SiN}_x\text{:H}$  coating is deposited (e.g. by plasma-enhanced chemical vapour deposition, PECVD). Front and rear contacts are formed by screen-printing of metal containing pastes (Ag for the front, Al for the rear

contact). A co-firing step in a belt furnace forms the Al-BSF by alloying, fires the Ag front contact through the  $\text{SiN}_x\text{:H}$  into the emitter region and releases atomic H from the layer into the Si bulk to passivate recombination active crystal defects. Edge isolation can be carried out e.g. by wet chemical etching, plasma etching or via laser which is not shown in Fig. 1. Cell parameters on standard Czochralski (Cz) large area solar cells are currently limited to around 18.4% for this screen-printing homogeneous emitter approach [1].

Current trends for further optimization of this homogeneous emitter approach are the development of pastes that can contact emitters with higher sheet resistance  $R_{sheet}$  [2] and/or the so-called seed-and-plate approach where a paste optimized for contacting high  $R_{sheet}$  emitters is used as a seed for an additional plating step which provides very good grid conductivity [3]. As these approaches may result in a narrower firing window or the application of an extra (plating) step, the formation of a selective emitter is a consequent alternative.

The selective emitter allows for the decoupling of the metalized and non-metalized front side areas. While for the contacted area via screen-printing a high doping

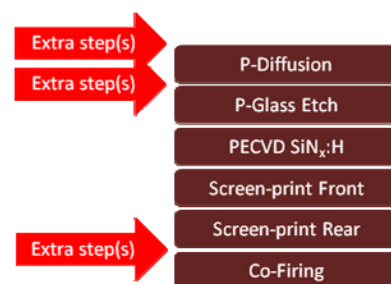


**Figure 1:** Standard processing scheme for homogeneous emitter solar cells (right) and possibilities for extra steps to be inserted in a selective emitter approach (details in the text).

concentration at the surface and a deep emitter is beneficial because of the resulting lower contact resistance and the wide firing window, the non-metalized areas need a lower doping level at the surface resulting in less (Auger) recombination and a better surface passivation. While the high doping underneath the contacts can result in a higher FF, the lower doping in the non-metalized areas results in a better blue response with higher  $j_{sc}$  and higher  $V_{oc}$  values due to a better surface passivation (and thinner or even no dead layer).

## 2.2 A brief history of selective emitters

Selective emitters are part of lab-type processes in order to reach very high efficiencies for a long time (see e.g. [4]). The first implementation into an industrial-type process was via the buried contact approach [5] which was commercialized by BP Solar. While higher efficiencies than for standard industrial-type screen-printed cells have been reached, the complexity of the process was a drawback, as the extra steps (e.g. laser groove formation, low pressure chemical vapour deposition of  $\text{SiN}_x$ , second diffusion at high temperatures, Ni/Cu plating) meant extra costs, and a non-standard cell fabrication line layout was needed. In addition, the high temperatures of the second P-diffusion did not allow for a hydrogenation of bulk defects via a  $\text{SiN}_x\text{:H}$  layer due to out-diffusion of H (apart from the fact that PECVD  $\text{SiN}_x\text{:H}$  exhibits pin holes in contrast to the more dense LPCVD  $\text{SiN}_x$  and therefore can cause parasitic plating). This process was therefore not suited for the processing of multicrystalline (mc) silicon solar cells.

From this experience some conclusions can be drawn. For successful implementation of a selective emitter process into industrial mass production, several aspects have to be considered which form a wish list:

- A minimum of extra steps
- Possibility of implementation into existing cell lines
- No yield losses (high stability and reliability)
- Higher efficiencies (also for mc Si)
- Higher efficiency not only on cell but also on module level

As a rule of thumb, efficiency should be increased by 0.2%<sub>abs</sub> for every extra step needed.

## 3 SELECTIVE EMITTER TECHNOLOGIES

Having in mind the points discussed above, several SE technologies have been developed within the last few years for the purpose of implementation in industrial mass production. In this section, several of them are presented, with the restriction to those which are already in production (or close to) and where recent published academic information is available. The list therefore might not be complete but is intended to serve as an overview of the various possibilities to realize a SE. Further restrictions are the full Al-BSF which allows compatibility with existing cell technology and the possibility to use screen-printing for front side contact metallization (although some of the presented technologies develop their full potential with alternative front side metallization like plating).

### 3.1 Doped Si inks

Innovallight Inc. developed a technology based on highly doped Si nano-particles which can be deposited

onto the Si wafer surface via screen-printing prior to P-diffusion [6]. Hereby the ink is deposited only in the areas where the screen-printed front contact is located afterwards. In the following P-diffusion step a lowly doped emitter is realized in the uncovered areas (80-100  $\Omega/\text{sq}$ ) whereas the areas with the highly doped Si nano-particles serve for contacting (30-50  $\Omega/\text{sq}$ ).

This technology adds only one additional step to the cell process prior to P-diffusion (see Fig. 1).

### 3.2 Oxide mask process

Centrotherm presented a SE technology based on a masked P-diffusion, where a thin  $\text{SiO}_2$ -layer slows down the diffusion of P-atoms from the surface into the Si bulk underneath the  $\text{SiO}_2$  [7]. The structuring of the  $\text{SiO}_2$  is done via laser ablation of the areas where the contacts are formed afterwards. A wet chemical etching step removes the damage induced by the laser. The heavily doped region (300  $\mu\text{m}$  wide) results in 45  $\Omega/\text{sq}$  and the masked area in 110  $\Omega/\text{sq}$ .

This technology offers a certain degree of freedom in emitter formation and uses technologies already established in PV.

### 3.3 Ion implantation process

Varian recently introduced a new technology for selective emitter formation based on ion implantation through a mask which reduces the implanted dose in the areas between the contacts [8]. An annealing step in oxidizing ambient is carried out for crystal damage removal caused during implantation and forms a thin  $\text{SiO}_2$ -layer on the wafer surface, which acts as surface passivation. The process continues with  $\text{SiN}_x\text{:H}$  deposition.

Advantages of this approach are the dry processing for emitter formation, the lack of P-glass formation (which normally has to be removed) and of junction isolation, as the emitter is formed only on the front side. In addition, the amount of process steps is not increased.

### 3.4 Etch-back process

University of Konstanz (UKN) developed an etch-back process which removes the dead layer of the heavily diffused regions after screen- or inkjet-printing of a mask covering the areas where the contacts are formed afterwards [9]. The etch-back is performed via the formation of porous Si and allows for a very sensitive and controllable removal of the first tens of nm as the porous Si formation is slowed down with increasing layer thickness almost independently of crystal orientation.

This process adds only one new tool, as the porous Si formation as well as etching of porous Si, P-glass and mask can be performed in the same (longer) wet bench already used for edge isolation. In addition it uses only existing technologies and is commercialized via Schmid.

### 3.5 Laser doping via P-glass

University of Stuttgart (IPE) introduced a laser-based SE technology, where the P-glass present after a 110  $\Omega/\text{sq}$  P-diffusion acts as P-source for the following laser process [10,11]. The laser with a special line-shaped beam profile melts the surface region in the areas for later front contact formation and the re-crystallized region is highly P-doped without crystal defects. The resulting profile (depth, peak surface concentration and  $R_{sheet}$ ) can be tailored by the laser pulse energy density.

This technology adds only one step and is commercialized via Manz. In addition, centrotherm is working on a similar approach as well [12].

### 3.6 Laser doping via LCP and NiAg LIP

One of the SE approaches developed at Fraunhofer ISE, now further studied at RENA, is based on simultaneous ablation of the PECVD SiN<sub>x</sub> layer and melting of the emitter layer underneath the ablated region (~120 Ω/sq) using a liquid-guided laser beam (laser chemical processing, LCP) [13]. The liquid contains P-atoms serving as P-source and heavy doping is reached after re-crystallization of the molten Si. The technology enables self-aligned light-induced plating (LIP) of the front contact e.g. via Ni and Ag.

Only one extra step is added and plating allows for thinner, highly conductive grid lines compared to screen-printed contacts.

### 3.7 Laser doping and plating

University of New South Wales (UNSW) developed a process similar to the one described in the previous section starting with a 100-120 Ω/sq diffusion [14]. Instead of the LCP the doping source can be e.g. phosphoric acid deposited on the wafer prior to laser doping. It allows for self-aligned plating of the front contacts as well. Both processes insert extra steps after firing of the Al-BSF, which can therefore be optimized independently of the front contact. In this approach a plated Ni/Cu/Ag front contact stack is used.

Two extra steps are added and the approach allows for thinner, highly conductive grid lines as well. Roth & Rau are working on commercialization.

### 3.8 IV results of SE technologies

Care has to be taken when results of the different SE technologies are compared. There are many critical issues that should be considered. Some of them are:

- differing cell formats
- different IV testers with different calibration cells
- Ag/Al pads on the rear side
- differing wafer resistivities
- Measurement before or after BO-related degradation (Cz Si)

**Table I:** IV results for SE technologies (B-doped Cz, full Al-BSF). Given are best cell IV parameters (left) and average efficiency values (right). The production line and the batch size are given as well.

\*: independently confirmed at ISE CalLab, \*\*: plated front contacts instead of screen-printing

SE technology	$j_{sc}$ [mA/cm <sup>2</sup> ]	$V_{oc}$ [mV]	FF [%]	$\eta$ [%]	size best/av. [mm]	$\eta_{av}$ [%] (line, batch size [cells])
Si Ink	37.5	637	79.0	18.9*	125/156	18.6 (JA Solar Production)
Oxide Diffusion Mask	37.2	634	79.2	18.7	156	18.6 (Pilot Line ct, ~50)
Ion Implantation	37.3	643	78.4	18.8	156	18.5 (Pilot Line Varian, 50)
Etch-back (por-Si)	37.9	640	78.4	19.0	125/156	18.5 (Sunrise Production)
Laser Doping (P-Glass)	37.0	637	78.9	18.6	156	18.5 (Pilot Line ct, ~50)
Laser Doping (LCP)**	37.3	633	80.3	19.0	156	n.a.
Laser Doping (P-Acid)**	37.8	639	77.8	18.8	156	18.5 (Pilot Line R&R, 5)

Nevertheless, some conclusions can be drawn from the results given in Tab. I.

The first striking fact is that the potential of all approaches reached so far seems to be very similar. For the best cells efficiencies are in the high 18% range, with typical values of  $j_{sc}=37.5$  mA/cm<sup>2</sup>,  $V_{oc}=640$  mV, FF=79% limiting efficiency to  $\eta=19.0\%$ . For the laser doping via LCP and phosphoric acid front contacts are fabricated by plating whereas for all other technologies standard Ag screen-printing was applied. The different technologies might not necessarily be totally optimized yet, but the main limitation for the IV parameters is the full Al-BSF at the rear side. Interestingly, first average efficiency data from industrial mass production lines and from pilot line processing at the equipment manufacturers seem to be very similar as well. Again, further optimization may lead to higher average values as well.

Compared to the efficiency potential of around 18.4% for a Cz Si solar cell with homogeneous POCl<sub>3</sub>-emitter using standard industrial-type processing as mentioned in section 2, an efficiency increase of 0.5-0.6% absolute is achieved with a selective emitter structure and the full Al-BSF as rear side contact.

## 4 EXAMPLE FOR SE EMITTER TECHNOLOGY: THE ETCH-BACK APPROACH

To highlight some important features of selective emitters in general, the etch-back selective emitter approach will be discussed as an example. In addition, some specialties of this technology will be addressed.

### 4.1 Features of etch-back emitters

Fig. 2 illustrates the principle of the emitter etch-back. The dead layer of a heavily diffused emitter is etched back until the desired phosphorous surface concentration [ $P_{surf}$ ] is achieved. The result is a relatively deep P-profile with a low [ $P_{surf}$ ] but still relatively low  $R_{sheet}$  which can not be reached by direct diffusion. In this way  $R_{sheet}$  and [ $P_{surf}$ ] can be decoupled to a certain degree and the emitter conductivity does not have to be increased, allowing the same front grid finger spacing without FF losses due to a higher series resistance.

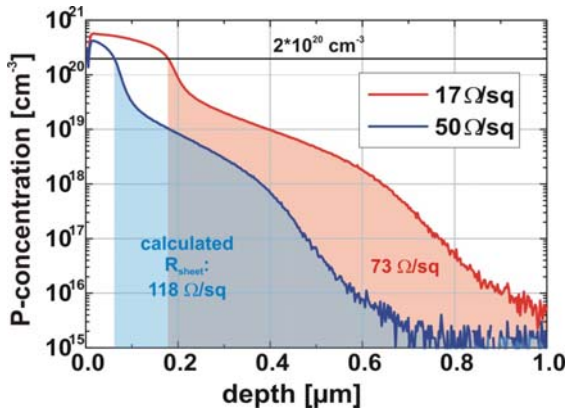


**Figure 2:** Principle of emitter etch-back with removal of the highly doped dead layer and the possibility of tailoring the doping profile by e.g. etching back to the same  $[P_{surf}]$  of  $2 \cdot 10^{20} \text{ cm}^{-3}$  resulting in different values for  $R_{sheet}$  (from [15]).

The lowering of  $[P_{surf}]$  reduces the emitter saturation current density  $j_{0E}$ . This can be seen in Fig. 3 where different directly diffused emitters are etched back step by step. As a result very low  $j_{0E}$  values can be reached independently of the starting  $R_{sheet}$  because  $j_{0E}$  is mainly influenced by  $[P_{surf}]$ .

As no high temperature steps exceeding the  $\text{POCl}_3$  diffusion temperature are involved, the etch-back selective emitter technology is also well suited for mc Si. A similar increase in efficiency of up to 0.5%<sub>abs</sub> has been observed and led to average values in industrial mass production of 17.1% (Sunrise production).

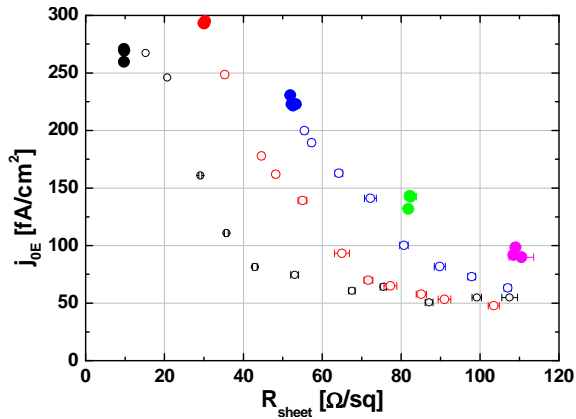


**Figure 3:** Lowering of  $j_{0E}$  (open symbols) with increasing etch-back of directly diffused  $\text{POCl}_3$ -emitters (solid symbols). The same low values for  $j_{0E}$  can be achieved by etching-back from different  $R_{sheet}$  starting values [16].

#### 4.2 $\text{POCl}_3$ versus inline emitter

For P-emitter formation two approaches are followed in industry. Apart from  $\text{POCl}_3$  diffusion in an open-tube furnace, inline diffusion in a belt furnace is done as well. Hereby a liquid P-source is deposited on the front wafer surface (e.g. by spray-on or spin-on), resulting in a single-sided diffusion with typically a higher  $[P_{surf}]$  due to higher diffusion temperatures and shorter diffusion times compared to  $\text{POCl}_3$  emitters. Therefore the blue response is normally lower for inline emitters. This can be seen in Fig. 4 where the effect of homogeneous and

selective emitters based on  $\text{POCl}_3$  and inline techniques are compared.

The improvement by etch-back is more pronounced for the inline emitter, reaching a similar quality as the homogeneous  $\text{POCl}_3$  emitter. But the higher short wavelength IQE is reached by the etched back  $\text{POCl}_3$  emitter.

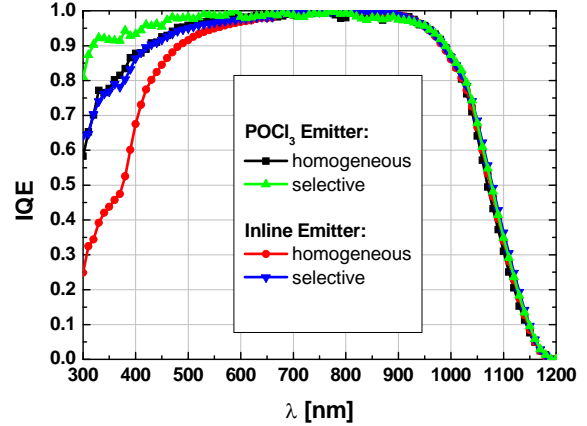


**Figure 4:** Comparison of homogeneous and selective emitters for inline and  $\text{POCl}_3$  techniques based on IQE. The improvement by etch-back is larger for the inline emitter [1].

#### 4.3 Effect of surface passivation

The lower doped part of selective emitters is more sensitive to surface passivation than a homogeneous emitter, mainly due to the lower  $[P_{surf}]$ . This effect is demonstrated in Fig. 5 by implied  $V_{oc}$  values of an emitter etched back from  $40 \text{ Ω/sq}$ . The emitter is covered with two different PECVD  $\text{SiN}_x\text{:H}$  layers differing in refractive index. The  $\text{SiN}_x\text{:H}$  with higher refractive index of  $n_{\text{SiN}}=2.15$  leads to higher implied  $V_{oc}$  values, especially for higher  $R_{sheet}$  (lower  $[P_{surf}]$ ). Therefore a stack system of PECVD  $\text{SiN}_x\text{:H}$  layers with a thin highly refractive and well passivating layer followed by a thick layer with standard refractive index can further increase surface passivation and cell performance [17].

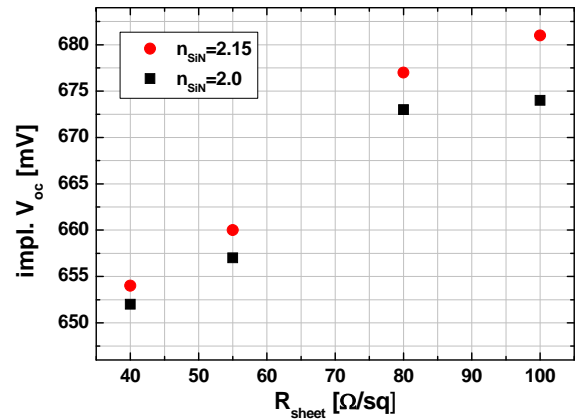


**Figure 5:** Dependence of implied  $V_{oc}$  on  $R_{sheet}$  for a  $\text{POCl}_3$  emitter etched back from  $40 \text{ Ω/sq}$ . A fired PECVD  $\text{SiN}_x\text{:H}$  layer with higher refractive index leads to higher implied  $V_{oc}$  values, especially with increasing  $R_{sheet}$  (lower  $[P_{surf}]$ ) [18].

#### 4.4 Effect of encapsulation

Selective emitters show an increase in IV parameters on cell level as demonstrated in Tab. I, but the enhanced performance has to occur on module level after encapsulation under glass as well. As part of the gain in short wavelength IQE might be lost due to absorption after encapsulation, experiments have been carried out to investigate this effect.

In Fig. 6 the transmission curves for pure module glass and EVA (ethylene vinyl acetate) under module glass are shown. It can clearly be seen that the EVA starts to limit the transmission at around 380 nm whereas the module glass transmits significantly shorter wavelengths. This negative effect of EVA concerning transmittance could be overcome by the use of alternative materials like silicones [19,20]. As shown in Fig. 6, the transmission of silicone under module glass is almost identical to the curve of the module glass alone. Therefore, encapsulation of solar cells under glass using silicones provides a better use of the short wavelength photons.

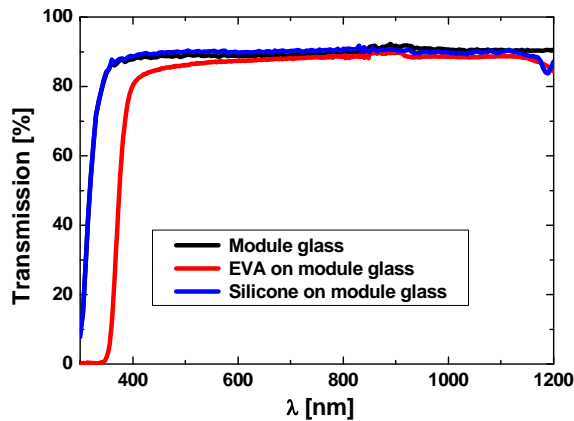


**Figure 6:** Transmission of module glass, EVA under module glass and silicone under module glass. Whereas EVA limits transmittance below 380 nm, silicone has a better transmission of short wavelength photons [19].

The better transmission of silicone results in a calculated gain in  $j_{sc}$  of almost  $0.4 \text{ mA/cm}^2$  as calculated in [19] for state of the art homogeneous emitter cells. This effect is demonstrated in Fig. 7 where a homogeneous emitter cell and a cell with selective emitter using etch-back technology are compared after encapsulation under EVA and under silicone. The loss in  $j_{sc}$  of around  $0.4 \text{ mA/cm}^2$  for the homogeneous emitter cell, calculated by the difference in IQE of the blue and black curve under AM1.5G, is only slightly higher for the selective emitter cell (green and red curves). The difference between the losses of the selective and homogeneous emitter cell can be roughly visualized by the area shaded in green and amounts to less than  $0.1 \text{ mA/cm}^2$ . Therefore, we can conclude that the additional loss of selective emitter cells by encapsulation under EVA compared to homogeneous emitter cells is almost negligible.

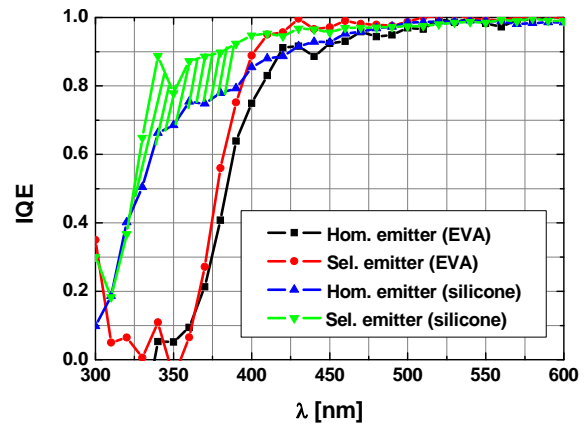


**Figure 7:** Effect of encapsulation of homogeneous and selective emitter solar cells under EVA and silicone. The area shaded in green visualizes the additional loss of a selective emitter solar cells ( $<0.1 \text{ mA/cm}^2$ ).

## 5 CONCLUSION AND OUTLOOK

Selective emitters allow a decoupling of metalized and non-metalized emitter areas and a separate optimization of both regions. The concept itself is rather old, but only one approach was implemented in rather standard industrial cell processing in the past (laser grooved buried contact). From this approach several lessons have been learned. The amount of extra steps (added complexity and cost), the place in the fabrication process where they are carried out, additional benefits (e.g. no extra steps, chance for self-aligned plating) and the efficiency increase that can be reached. Seven technologies have been presented (doped Si inks, oxide masking process, masked ion implantation, etch-back by formation of porous Si, laser doping via P-glass, laser doping via LCP, laser doping via phosphoric acid), and their current status concerning IV results was given.

Recently several groups introduced selective emitter concepts for standard screen-printing based solar cell technology (full Al-BSF). These approaches can be distinguished by the amount of extra steps (added complexity and cost), the place in the fabrication process where they are carried out, additional benefits (e.g. no extra steps, chance for self-aligned plating) and the efficiency increase that can be reached. Seven technologies have been presented (doped Si inks, oxide masking process, masked ion implantation, etch-back by formation of porous Si, laser doping via P-glass, laser doping via LCP, laser doping via phosphoric acid), and their current status concerning IV results was given.

The efficiencies demonstrated for best cells are all pretty consistent and the current limit of around 19.0% for all technologies (Cz Si) seems to be given by the full Al-BSF at the rear. For two technologies (doped Si ink and etch-back by porous Si) IV data from industrial mass production are available and average efficiencies of 18.5-18.6% have been reached already.

As an example the etch-back technology was used to highlight some features of selective emitters. While inline emitters benefit more from the selective emitter concept, higher absolute efficiencies can be reached for  $\text{POCl}_3$  emitters.

The etch-back process decreases the phosphorous surface concentration while maintaining a deep and relatively low  $R_{sheet}$  emitter. This allows for a significantly better surface passivation, which can even be further improved by the use of PECVD  $\text{SiN}_x\text{:H}$  layers with higher refractive indices. This technology even

works for mc Si and an average efficiency in industrial mass production of 17.1% has been reached.

Encapsulation under module glass and EVA cuts off the short wavelength photons due to absorption in the EVA. Silicones could be an alternative to avoid the loss of 0.4 mA/cm<sup>2</sup> for homogeneous emitter cells. The loss for selective emitter cells is slightly higher, but the additional loss in  $j_{sc}$  can be estimated to be <0.1 mA/cm<sup>2</sup> and is therefore almost negligible.

The full potential of selective emitters with their low  $j_{0E}$  values can be exploited when improved rear side concepts will be available for industrial application.

## 6 ACKNOWLEDGEMENTS

The author would like to thank various people from all the institutes mentioned in the paper for their input concerning their selective emitter technology. In particular F. Book and A. Dastgheib-Shirazi contributed with recent results on the etch-back approach.

## 7 REFERENCES

- [1] F. Book, unpublished
- [2] A. Ebong, A. Rohatgi, W. Zhang, M. Neidert, Understanding the role of glass frit in the front Ag paste for high sheet resistance emitters, Proc. 22<sup>nd</sup> EU PVSEC, Milan 2007, 1734
- [3] M. Hörteis, S.W. Glunz, Fine line printed silicon solar cells exceeding 20% efficiency, Progr. Photovolt.: Res. Appl. **16**(7) 2008, 555
- [4] J. Zhao, A. Wang, P. Altermatt, S.R. Wenham, M.A. Green, 24% efficient PERL silicon solar cell: Recent improvements in high efficiency silicon cell research, Sol. En. Mat. and Sol. Cells **41/42** (1996) 87
- [5] S. Wenham, Buried-contact silicon solar cells, Progr. Photovolt. Res. Appl. **1**(1) (1993) 3
- [6] H. Antoniadis, F. Jiang, W. Shan, Y. Liu, All screen printed mass produced silicon ink selective emitter solar cells, Proc. 35<sup>th</sup> IEEE PVSC, Honolulu 2010
- [7] A. Esturo-Breton, F. Binaie, M. Bresselge, T. Friess, M. Geiger, E. Holbig, J. Isenberg, S. Keller, T. Kühn, J. Maier, A. Münzer, R. Schlosser, A. Schmid, C. Voyer, P. Winter, K. Bayer, J. Krümborg, S. Henze, I. Melnyk, M. Schmidt, S. Klingbeil, F. Walter, R. Kopecek, K. Peter, Crystalline silicon solar cells with selective emitter for industrial mass production, Proc. 24<sup>th</sup> EU PVSEC, Hamburg 2009, 1068
- [8] R. Low, A. Gupta, N. Bateman, D. Ramappa, P. Sullivan, W. Skinner, J. Mullin, S. Peters, H. Weiss-Wallrath, High efficiency selective emitter enabled through patterned ion implantation, Proc. 35<sup>th</sup> IEEE PVSC, Honolulu 2010
- [9] H. Haverkamp, A. Dastgheib-Shirazi, B. Raabe, F. Book, G. Hahn, Minimizing the electrical losses on the front side: development of a selective emitter process from a single diffusion, Proc. 33<sup>rd</sup> IEEE PVSC, San Diego 2008
- [10] S.J. Eisele, T.C. Röder, J.R. Köhler, J.H. Werner, 18.9% efficient full area laser doped silicon solar cell, Appl. Phys. Lett. **95** (2009) 133501
- [11] T.C. Röder, S.J. Eisele, P. Grabitz, C. Wagner, G. Kulshich, J.R. Köhler, J.H. Werner, Add-on laser tailored selective emitter solar cells, Progr. Photovolt. Res. Appl. (2010) DOI: 10.1002/pip.1007
- [12] T. Friess, A. Esturo-Breton, F. Binaie, M. Bresselge, M. Geiger, J. Isenberg, S. Keller, T. Kühn, J. Maier, A. Münzer, A. Schmid, C. Voyer, P. Winter, W. Zimmermann, K. Bayer, S. Henze, S. Hüls, W. Kästle, J. Krümborg, I. Melnyk, C. Rasz, M. Schmidt, F. Walter, R. Kopecek, K. Peter, L. Hildebrand, M. Müller, P. Fath, Selective emitter on crystalline Si solar cells for industrial high efficiency mass production, this conference
- [13] D. Kray, N. Bay, G. Cimiotti, S. Kleinschmidt, N. Kösterke, A. Lösel, M. Sailer, A. Träger, H. Kühnlein, H. Nussbaumer, C. Fleischmann, F. Granek, Industrial LCP industrial emitter solar cells with plated contacts, Proc. 35<sup>th</sup> IEEE PVSC, Honolulu 2010
- [14] B. Tjahjono, S. Wang, A. Sugianto, L. Mai, Z. Hameiri, N. Borojevic, A. Ho-Baillie, S.R. Wenham, Proc. 23<sup>rd</sup> EU PVSEC, Valencia 2008, 1995
- [15] F. Book, A. Dastgheib-Shirazi, B. Raabe, H. Haverkamp, G. Hahn, P. Grabitz, Detailed analysis of high sheet resistance emitters for selectively doped silicon solar cells, Proc. 24<sup>th</sup> EU PVSEC, Hamburg 2009, 1719
- [16] F. Book, T. Wiedenmann, A. Dastgheib-Shirazi, B. Raabe, G. Hahn, Large area n-type silicon solar cells with selective front surface field and screen printed aluminum-alloyed rear emitter, this conference
- [17] A. Dastgheib-Shirazi, F. Book, H. Haverkamp, B. Raabe, G. Hahn, Investigations of high refractive silicon nitride layers for etched back emitters: Enhanced surface passivation for selective emitter concept (SECT), Proc. 24<sup>th</sup> EU PVSEC, Hamburg 2009, 1600
- [18] H. Haverkamp, Kristalline Silizium-Solarzellen mit selektiver Emitterstruktur: Entwicklung, Implementierung und Potential einer zukunftsweisenden Technologie, Dissertation, University of Konstanz, 2009
- [19] S. Ohl, G. Hahn, Increased internal quantum efficiency of encapsulated solar cells using two-component silicone as encapsulant material, Proc. 23<sup>rd</sup> EU PVSEC, Valencia 2008, 2693
- [20] B. Ketola, K.R. McIntosh, A. Norris, M.K. Tomalia, Silicones for photovoltaic encapsulation, Proc. 23<sup>rd</sup> EU PVSEC, Valencia 2008, 2969